The College of Engineering
University of Wisconsin-Madison

Wisconsin Electric Machines and Power Electronics Consortium

RESEARCH REPORT
92-26

A Completey Isolated Three-Phase to Three-Phase Induction Motor/Induction Generator Power Conversion System

I. Alan, T. Lipo
Dept. of Elec. and Comp. Engr.
University of Wisconsin-Madison
1415 Johnson Drive
Madison, WI 53706

WEMPEC

Department of Electrical and Computer Engineering
1415 Johnson Drive
Madison, Wisconsin 53706

A Completely Isolated Three-Phase to Three-Phase Induction Motor/Induction Generator Power Conversion System

Irfan Alan Thomas A. Lipo

University of Wisconsin
Electrical and Computer Eng. Dept.
Madison Wisconsin

Abstract - Two squirrel cage induction machines interconnected via a parallel resonant high frequency AC link and associated switching Pulse Density Modulated (PDM) converters are investigated, one operating as a generator and the other as a motor. No capacitors are used for the excitation of the generator or motor. Instead, the real power of the generator is controlled so as to maintain the proper link voltage and match the power between the input and output. Since the source (induction generator) does not have a constant voltage and frequency, the control of the system is much more complex compared to the utility type source. Current regulated PDM converters operating via field oriented controllers are used to control both induction machines. A zero voltage switching technique is utilized with the associated PDM converters. Low harmonic distortion waveforms has been obtained both at the input and output due to the 40 kHz high switching frequency. Link voltage build-up and regulation techniques are investigated. Computer simulations demonstrates the feasibility of the proposed system.

I. Introduction

For aviation and space station applications, a 60 Hz utility grid becomes impractical because of the size of the magnetic components. A 20 kHz high frequency AC link has been proposed as a typical utility for these type of applications as a means of obtaining high power densities [Watts/kg] and for flexibility in accomplishing voltage level changes. There is also a growing tendency of using high frequency induction machines in actuator motor control for orbiting and flight control applications for similar reasons.

Over the past several years, research activities at the University of Wisconsin have focused on the development of a high frequency ac link power conversion system for this purpose [1-11]. The high frequency ac link converter is a significant advance in the state of the art in power converter technology since it more optimally utilizes the capabilities of the power switching device by turning devices on or off only when the voltage across the device is nearly zero. Hence, the switching frequency of the power converter can be increased by an order of magnitude while, at the same time, reducing the converter losses. During the past several years a complete double bridge ac link system has been constructed. The double bridge permits the electrical machine to operate at variable frequency with full bidirectional power flow in either rotational direction. The operation of a squirrel cage induction machine operating under closed loop speed and torque control utilizing the field oriented control principle has been investigated. Both motoring and generating operation was examined and full reversibility of the direction of rotation of the induction machine has been demonstrated in hardware [3]. The drive can be operated as an ac dynomometer providing rapid torque response in all four quadrants of operation.

The existing experimental breadboard consists of a three phase to three phase power converter and induction machine drive system accepting/delivering power from/to three phase 60 Hz utility grid based upon a PDM converter utilizing 20 kHz parallel resonant HF (high frequency) AC link technology. This system is capable of driving the induction machine of the system as an AC dynamometer up to the power range of 10 hp (7.46 kW) and speed range of 9,000 rpm [10]. An 18,000 rpm speed range can also be achieved by replacing the current regulator from "Direct ON-OFF" to a "Mode Controller" control strategy reported in references [3,6] and by rescaling some of the control circuit quantities.

When the induction machine is operated as a generator, the power generated by machine can be used to drive second induction machine rather than delivering it back to the 60 Hz utility source at unity power factor. This new concept is the subject of the study of this paper. In effect, it will be shown that the induction machine of the system can be operated as a generator and the three phase 60 Hz utility replaced by second induction machine. In such a case it is clear that, the real power control between the two machines via a parallel resonant HF AC link becomes a challenging problem. This problem is studied in detail through the computer simulations to develop a general insight concerning the application of high frequency link systems to isolated systems [11]. A computer program was developed and many computer simulations were carried out wherein the full dynamics of the two induction machines were considered. Two field oriented controllers are used to control both induction machines. One of the controllers manages the load side machine dynamics and the other regulates the link voltage by balancing the power transfer between input and output. Since the flow of power from one side of the link to the other is managed by means of the two field oriented controllers, no power factor correcting capacitors are used for the excitation of either the generator or motor. Both of the induction machines can be fully operated in four quadrants when necessary.

II. Overall Operating Principle of the System

2.1 Starting Operation

A simple block diagram of the proposed system is shown in Fig. 1. The overall operation principle of the system can be briefly described as follows. Initially the starting of the overall system is achieved via an initial charging circuit. Since no additional excitation capacitors are needed for the excitation of the induction generator, the required excitation

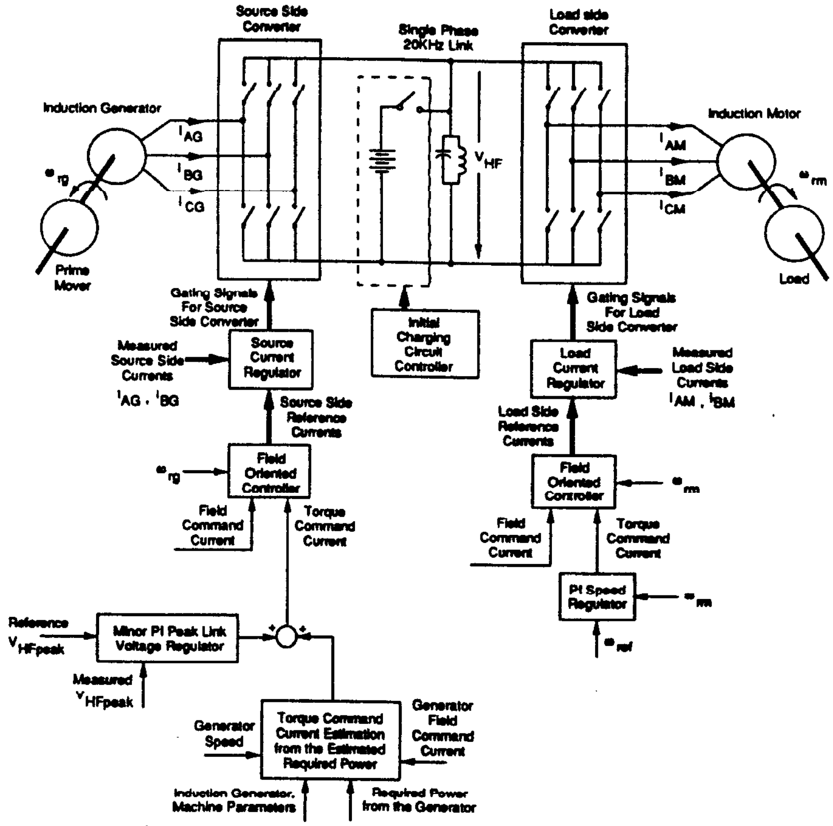

Fig. 1. Power Circuit and System Control Block Diagram of Completely Isolated 3Ø to 3Ø Power Conversion System.

must be achieved via operation of the source side PDM converter and the parallel resonant AC link. At the starting instant, the link voltage is zero and induction generator is not excited implying that induction generator can not supply active power as a source even if it is given a torque command. Therefore, an initial charging circuit is needed both to establish the link voltage and to excite the induction generator initially. Such an initial charging circuit diagram is shown in Fig. 2. This circuit is operated until a sufficient flux level is established inside the generator.

In order to establish a flux inside the induction generator as soon as possible and take full advantage of the instantaneous power circulating inside the machine only a flux component current command is applied via the field oriented controller. In other words, until a sufficient level of flux is established inside the generator the 3Ø currents circulating inside the machine are only comprised of their flux components. To establish such a level of flux inside the induction generator depending on the size and the ratings of the machine can take several hundred milliseconds. Once a sufficient flux level is established inside the generator, the initial chaarging circuit is disconnected from the system leaving the control of the power of the system only to the induction generator torque command estimator. This condition, in turn, implies that the peak link voltage regulation is solely left to the torque command estimation of the generator during normal operation.

2.2 Operation of the Initial Charging Circuit

The power circuit of the initial charging circuit which is used to build-up HF resonant peak link voltage and establish a flux inside the generator is shown in Fig. 2. The operation principle of this circuit depends on the control of two quantities one of which is the HF peak link voltage level and the other is the current level in the inductor used in this initial charging circuit. As seen in Fig. 2. only a single switch which has unilateral current carrying and bilateral voltage blocking capability is used to control the power flow from the initial charging circuit to the main system.

The operating principle of this initial charging circuit can be briefly explained as follows. Initially, upon receiving a start command, the switch which allows power transfer from the initial charging circuit to the main system is turned on, therefore allowing a certain amount of peak link voltage build up. Later, when the current level in the inductor is less

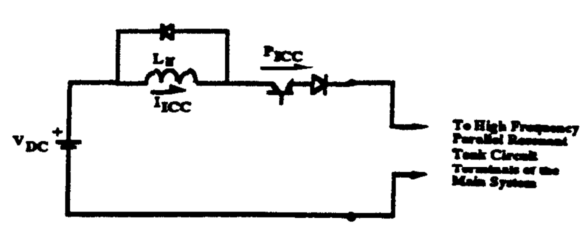

Fig. 2. Power Circuit Layout of Initial Charging Circuit.

than a specified value and the peak link voltage is less than its reference, the incoming negative HF link voltage half cycle which will support the current flow in the inductor is selected, otherwise the switch remains off. When the current level in the same inductor is greater than the specified value and the peak link voltage is less than its reference, then the incoming positive HF link voltage half cycle which will impede the current flow in the inductor is selected. Otherwise the switch remains off. When the peak link voltage is greater than its reference, the switch is kept off until it becomes less than its reference.

Using this approach, the flux inside the induction generator can be established via the parallel resonant 20 kHz AC link and the generator side PDM converter. Here, the peak link voltage is regulated by the initial charging circuit. As stated earlier, the time required for the excitation of the induction machine needed to generate the required active power by solely induction generator varies with size. For the 10 hp induction generator whose ratings are given in Section III, this time is determined through the computer simulations to be about 150 msecs. Therefore, the initial charging circuit used to boost and maintain the resonant link voltage and excite the 10 hp induction generator requires approximately a 225 Wsec energy delivery capacity or with 120 V dc source voltage, a 1.875 Amp-sec current delivery capacity.

2.3 Power Balance Between Input and Output

The management of the real power between the two machines via a parallel resonant high frequency AC link is clearly a challenging control problem. Specifically, the real power of the generator has to be controlled so as to maintain the proper link voltage while maintaining a match between the power of the input and output. Since power matching on an instantaneous basis is not possible, an average power matching technique which makes use of power estimation for both side induction machines has been utilized. The converter and resonant tank circuit losses which constitute the major part of the power required from the source when the system is operated at low power levels is also incorporated to the estimation of the required power from the generator. An instantaneous power difference between the instantaneous and estimated average power is handled via the resonant tank circuit energy storage capacity and a minor PI peak link voltage regulation loop.

2.4 Estimation of the Torque Command of the Induction Generator.

To be able to estimate the torque component current comand of the induction generator the required power from the generator must first be specified. There are two main portions of the estimated power required from the induction generator. One part of this estimation includes the average induction machine power corresponding to the load machine. The other part includes the total operating losses of the system, namely the HF parallel resonant tank circuit losses, PDM converter losses and load machine losses.

2.4.1. Estimation of the Average Load Machine Power

Estimation of this quantity is determined via measurement of the terminal quantities of the load machine and a filtering process. Measured and filtered load machine power termed MPWRF is defined as

$$MPWRF=Filter\{v_{as}i_{as}+v_{bs}i_{bs}+v_{cs}i_{cs}\}.$$

A low pass second order butterworth filter with a 500 Hz corner frequency and a 0.707 damping factor is used to filter the measured instantaneous active power of the load machine. This process yields an average active power estimation of the laod machine on an almost instantaneous basis.

2.4.2. Estimation of the HF Parallel Resonant Tank Circuit Losses

A fictitious loss resistor parallel to the link is defined for the operational losses of the HF parallel resonant tank circuit. Depending upon the peak value of the HF link voltage and the number of parallel resonant tank circuits paralleled, the estimation process can be carried out by supposing that an individual tank circuit has an equivalent impedance of Z_T and a fictitious loss resistor of r_T. The average loss is defined in terms of the HF peak link voltage value, V_{HFpeak}, as follows:

$$P_{HFL} = n\, r_T \left(\frac{V_{HFrms}}{Z_T}\right)^2 \quad (1)$$

where "n" is the number of equivalent paralleled resonant tank circuits and

$$V_{HFrms} = \frac{V_{HFpeak}}{\sqrt{2}} \quad (2)$$

2.4.3. Estimation of the PDM Converter Losses

The major part of these losses are constituted by the converter conduction losses. The switching losses are neglected because of their insignificant magnitude due to the use of resonant link technology. The estimation of the conduction converter losses for each individual 3Ø PDM converter is accomplished via the following procedure. Since only one single device is in conduction in a single branch of the bridge at any time, there are only three devices conducting at a time in one bridge. Since these three switches are carrying 3Ø currents, the negative of the algebric summation of the two currents carried by two different switches gives the third switch current at any given time. Therefore, the average converter conduction losses for a 3Ø bridge on an instantaneous basis can be approximately calculated as follows:

$$P_{CCL}=2 \times (V_{FWD} \times (|IAS|+|IBS|)) \quad (3)$$

where P_{CCL} is the converter conduction losses, V_{FWD} is the forward voltage drop of each bidirectional switch in conduction, $|IAS|$ and $|IBS|$ are the absolute values of the currents carried by the two different switches of two different braches of the specified 3Ø bridge.

2.4.4. Load Machine Losses

Since both induction machines are controlled via current regulated indirect field oriented controllers, the known dc torque and flux component current commands and the measured speed of the machine helps in determining the operational losses of the machines. Since both machines are controlled so as to keep V/f constant, the iron losses of the machines become proportional to speed. Therefore, knowing flux and torque component current commands helps to determine the copper losses and knowledge of the speed information helps to determine the iron losses.

2.4.5. Estimation of the Total Average Required Active Power from the Induction Generator

The algebric summation of above four estimated average powers on an instantaneous basis gives the total required power from the induction generator. If this power is defined as P_{REQ}, then the estimation of the torque component current command of the generator is realized by using the steady state torque equation defined in synchronous reference frame for the field oriented induction machine. That is

$$T_e^{ss} = \frac{3}{2}\,\frac{P}{2}\,\frac{L_m^2}{L_r}\, i_{ds}^{ess}\, i_{qs}^{e} \qquad (4)$$

where i_{ds}^{ess} denotes the steady state value of current required to magnetize the machine and hold constant rotor flux. The superscript "ss" is used for this quantity since it is always maintained as constant. The transient state model in a synchronous reference frame is used to derive the above equation. In other words, the reference axes are assumed to be rotating at synchronous speed, ω_e.

In addition to the electrical torque equation, speed information for the induction generator is needed in order to estimate the required torque component current command. Therefore, assuming that mechanical rotor speed is measured and known then the average induction machine power can be defined as:

$$P_{av} = T_e^{ss}\ \omega_{rg} \qquad (5)$$

where ω_{rg} is the angular velocity of the rotor in radians per second.

Using Eqs. 4 and 5, the torque component current command of the generator can now be estimated as follows:

$$i_{qsg}^{e*} = \frac{2}{3}\, P_{REQ}\, \frac{L_{rg}^{*}}{(L_{mg}^{*})^2\, \omega_{reg}\, i_{dsg}^{e*ss}} \qquad (6)$$

where subscript "g" stands for generator quantities.

In general, there inevitably will be a difference between the instantaneous and estimated average powers. Hence, peak link voltage variations are observed on an instantaneous basis and controlled to ensure that the link voltage amplitude is ensured. As mentioned earlier, this difference is handled by the energy storage capacity of the resonant tank circuit. The higher the energy storage capacity, the lesser the peak link voltage variations, yet the higher the losses and weight. A proportional-integral peak link voltage regulator is included as a minor loop to the estimation of the same torque command to prevent excessive peak link voltage variations. A block diagram of the overall torque command estimator for the induction generator is given in Fig. 3.

III. Computer Simulation Results

Initial computer simulations of this system have been done based on a 10 Hp, 230 V, 32 A, 300 Hz, 6-pole induction generator and a 2 Hp, 208 V, 10 A, 400 Hz, 8-pole induction motor (Subsequently replaced by a 10 Hp machine in a later phase of study).

The name plate ratings and equivalent circuit parameters of induction generator which was simulated are given as follows:

3 phase (3Ø), 10 Hp (7.46 kW), 230 V, 32 A.
300 Hz, 6 poles 6000 rpm @ no load, 5957 rpm @ rated torque.
Δ-Connected Stator Winding.
Squirrel Cage Rotor Designed to Operate at 900 Hz (18,000 rpm) with Field Weakening.
r_{1dc} =0.195 Ω, r_2' =0.10482 Ω.
r_M =240 Ω @ 300 Hz and 40.411 Ω @ 60 Hz.
$L_{1l} = L_{2l}'$=0.6796 mH with Measurement at 60 Hz.
L_M =11.149 mH at 300 Hz and 10.888 mH at 60 Hz.
S_R =0.0072 @ 230 V_{ll}/300 Hz V/f Ratio and Rated Torque Operation.
S_R =0.0358 @ 46 V_{ll}/60 Hz V/f Ratio and Rated Torque Operation.

It is worthwhile to mention here that the equivalent circuit parameters given represent per phase quantities for a Δ-connected stator winding. In the computer simulations, fictitious per phase equivalent circuit parameters for Y-connected stator winding are used.

As for the induction motor used at the output side of the converter, it has the following nameplate ratings and equivalent circuit parameters per phase for Y connected stator winding:

3Ø, 208 V, 10 A, 2 HP, 400 Hz, 8 pole, 5600 rpm
r_1 =0.45 Ω, r_2 = 1.036 Ω,
L_M = 5.98 mH, $L_{lr} = L_{ls}$ = 0.656 mH

An inertia of J = 0.01 Nmsec^2 and 0.0 damping coefficient is assumed.

When the load machine is replaced by a 10 Hp machine in the simulations, the induction machine which has the following name plate ratings and equivalent circuit parameters is used.

3 phase (3Ø), 10 Hp (7.46 kW), 230 V/460 V
24.2 A/12.1 A, 60 Hz, 4 poles.
1800 rpm @ no load, 1750 rpm @ rated torque
Star-Connected Stator Winding, Squirrel Cage Rotor.
r_{1dc} =0.1844 Ω, r_2' =0.2009 Ω,
r_M =197.89 Ω @ 60 Hz and @ 230 V,
r_M =113.98 Ω @ 60 Hz and @ 115 V,

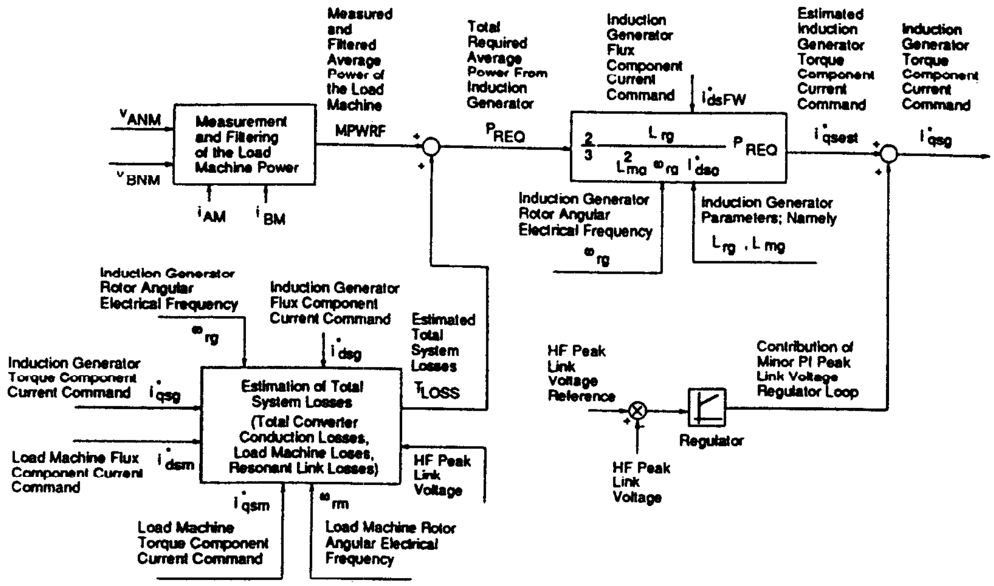

Fig. 3. Block Diagram of the Torque Component Current Command Estimator of the Induction Generator.

r_M =33.007 Ω @ 60 Hz and @ 50 V,
$L_{l1} = L_{2l}'$=1.4345 mH with Measurement at 60 Hz,
L_M =37.577 mH at 60 Hz and 230 V,
L_M =38.598 mH at 60 Hz and 115 V,
L_M =35.448 mH at 60 Hz and 50 V,
S_R =0.02777 @ 230 V_{ll}/60 Hz and Rated Torque Operation.

As for the parallel resonant tank circuit parameters, a 22.5 μH resonant tank circuit inductor and a 3.0 μF resonant tank circuit capacitor are assumed as individual tank circuit parameters. The number of paralleled resonant tank circuits are assumed to be three. A fictitious loss resistor r_T of 0.02 Ω is assumed per tank circuit and corresponds to a loss of approximately 350 W per resonant tank circuit for a 500 V peak link voltage operation.

3.1 Starting of the System by Initial Charging Circuit and Link Voltage Build-up.

Figure 4 shows the start up of the system by the initial charging circuit. To establish a flux inside the induction generator as soon as possible and take full advantage of the circulating instantaneous power inside the machine, only the rated flux component current command is applied to the machine via the indirect field oriented controller. The time trace in this figure shows a range from 0 to 20 msec. As can be seen, the peak link voltage reaches its reference within a millisecond and the flux continuously builds up inside the generator. The phase A line current of the induction generator is composed only of its flux component and is quite well regulated via the PDM converter and field oriented controller. The terminal voltage of the machine also builds up as flux inside the generator reaches toward its reference. The terminal voltage shown in the figure is a filtered quantity to enable phase more clearly. An initial charging circuit dc source voltage is chosen to be 120 V as seen from the figure. The current I_{icc} of the initial charging circuit represents the

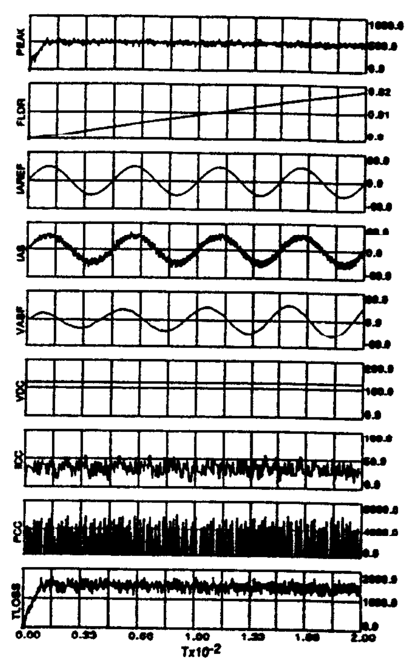

Fig. 4. Link Voltage and Generator Flux Build-up by Initial Charging Circuit. From the Top: **PEAK:** Peak HF Link Voltage–V. **FLDR:** Generator Rotor Flux d-axis Component in Synchronous Reference Frame-Vsec. **IAREF:** Generator Phase A Line Current Reference–A. **IAS:** Generator Phase-A Line Current-A. **VASF:** Filtered Phase-A Generator Line to Neutral Voltage–V. **VDC:** Initial Charging Circuit DC Source Voltage–V. **IICC:** Initial Charging Circuit Inductor Current in A. **PICC:** Power Transferred from Initial Charging Circuit to Main System–W. **TLOSS:** Total Loss of the Resonant Tank and PDM Converter–W. Time/div:1.000 msec.

inductor current shown in Fig. 2. Thus the constant current intervals refer to the freewheeling of the current through the diode paralleled to the inductor. As it can be noted, in these time intervals there is actually no power transfer from the initial charging circuit to the main system. The major part of the power required from the initial charging circuit is spent as losses in the system since no subsequent torque command is applied to the induction generator. The resonant tank circuit constitutes a large portion of these losses with around 1000 W and the remainder is essentially the converter conduction losses.

Figure 5 shows the start of active power generation by the induction generator at the time instant 150 msec. Removal of the initial charging circuit occurs at the same time instant. A sufficient level of flux inside the generator allows the induction generator to take over and supply the required power with the proper torque command that has been estimated. At the end of the time scale shown in the figure, the machine flux and terminal voltages are about to reach their rated values. The line to line induction generator terminal voltage shown in this figure is again a filtered quantity. The torque command, developed torque, estimated average induction generator power and real average induction generator power are also shown in this figure. Even though the torque command is zero for the first 150 milliseconds, there is a high frequency torque ripple developed in the machine whose average value is zero probably owing to the high frequency current ripple in the actual current. The negative average torque and power developed by the generator and zero power transfer from the initial charging circuit to the main system after 150 msec shows the feasibility of operation of this system in a completely isolated manner. The load side induction motor is operated at 200 msec and the slight jump in the total losses at the same instant is a result of this change in operation.

3.2 Performance Analysis of the Induction Motor Operating from a Completely Isolated 3Ø to 3Ø Converter:

Figure 6 shows the load side PDM converter and the induction motor starting at 200 msec. The induction motor is operating in the speed regulation mode via a current regulated indirect field oriented controller which has been given a speed reference of 4000 rpm. The two HP load machine reaches to its speed reference at approximately 200 msec with full torque command applied. As soon as the load machine reaches its speed reference, the torque command of the machine drops to nearly zero since there is no load torque applied at that moment. Furthermore, the command stays negative for some time because of the overshoot in the actual speed. Later, the speed of the motor is still well regulated to its reference when a load torque is applied and removed. While all of these events are taking place, the induction generator is given a proper torque command which produces a proper amount of average torque and power yielding a quite well regulated HF peak link voltage.

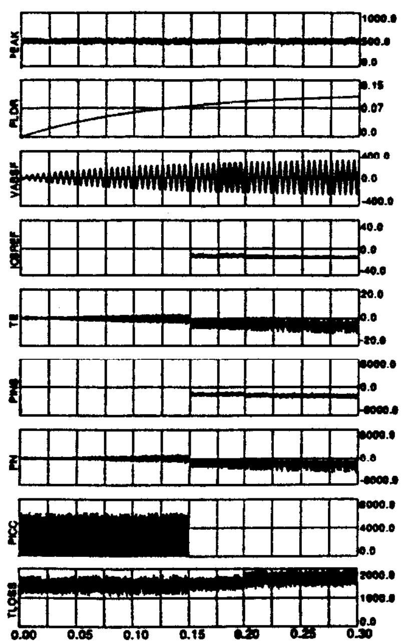

Fig. 5. Induction Generator Flux Build-up, Disconnection of Initial Charging Circuit and Subsequent Power Balancing/ From the Top: PEAK: Peak of the HF Link Voltage in V. FLDR: Generator Rotor Flux d-axis Component-Vsec. VABSF: Filtered Phase-AB Generator Line to Line Voltage-V. IQSREF: Generator Torque Component Current Command-A. TE: Average Electrical Torque of Induction Generator-Nm. PINE: Estimated Average Generator Power-W. PIN: Average Generator Power in W. PICC: Power Transferred from Initial Charging Circuit to the Main System-W. TLOSS: Total Loss of Resonant Tank and PDM Converter-W. Time/div: 25 msec.

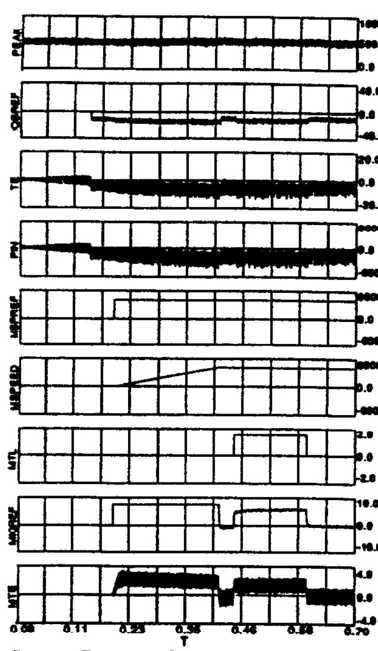

Fig. 6. Dynamic Response of System to Speed and Load Torque Changes. From the Top: PEAK: Peak of HF Link Voltage-V. IQSREF: Generator Torque Component Current Command-A. TE: Average Electrical Torque Developed by Generator-Nm. PIN: Average Generator Power-W. MSPREF: Induction Motor Speed Reference -rpm. MSPEED: Speed of Induction Motor-rpm. MTL: Induction Motor Load Torque-Nm. MIQREF: Motor Torque Component Current Command-A. MTE: Average Electrical Torque of Induction Motor-Nm. Time/div: 58.333 msec.

Figure 7 shows the response of the induction motor and overall system to a change in speed command. The HF peak link voltage and the power balance between the input and output is well regulated while the induction motor is going through each phase of full four quadrant operation. The simulation results presented here clearly demonstrates the feasibility of operation of the proposed system.

3.3 Performance of System When 2 HP Load Machine is Replaced by 10 HP Machine.

To show higher power generation capability of the induction generator under a similar type of operation, a higher power load machine and a 6000 rpm generator speed has been simulated in software. When the speed of the induction generator is increased from 4000 rpm to 6000 rpm, the peak link voltage regulation becomes poor because of the higher back emf voltage of the generator. To eliminate this problem, the peak link voltage was increased to 700 V and subsequently good regulation was obtained.

The software simulation results presented in Figs. 8 through 10 show the performance of this, more highly loaded, system. The starting and normal operation of the system is the same as described for the 2 HP load machine case. Similar type of arguments apply for the interpretation of the figures. One significant diference is that a full torque component current step command now can not be applied to the load machine at its rated speed at which case the sum of all the average active power required from the generator exceeds the power supply capability of the induction generator.

In order to not limit the torque command of the load machine to a lower value during all times of operation, the torque command of the induction generator can be observed such that whenever the induction generator nears the limit of its power supply capability, the torque command of the load machine is reduced to a predetermined lower value to reduce the power demand. Such action prevents the induction generator from going beyond the limits of its capability and causing a problem in the control of proper peak link voltage. Such a preventative measure can be observed from Figs. 8 and 9. At the instant approximately t=1.05 sec., the load machine begins to demand roughly 5 kW from the generator. The addition of the load machine losses, converter losses, and high frequency resonant tank circuit losses brings the power demand to the edge of the power supply limit of the induction generator. Therefore, the torque component current command of the load machine must be regulated back and forth to a predetermined lower value to prevent the appearance of undesirable control problems. Control strategies to help predict and avoid such situations is presently being explored.

IV. Conclusions

This paper has demonstrated the feasibility of a completely isolated induction motor-induction generator 3Ø to 3Ø power conversion system. The machines are both supplied from a 20 kHz parallel resonant ac link via associated Pulse Density Modulated (PDM) converters and receive their excitation solely by means of field oriented control. Fast dynamic changes of the load are handled by the overall system controller by properly matching the input and output powers and at the same time regulating the high frequency peak link voltage properly.

Computer simulations demonstrate the feasibility of a hardware prototype implemetation of the proposed system. Experimental results for this system are in the process of being obtained and will be reported as part of the paper presentation.

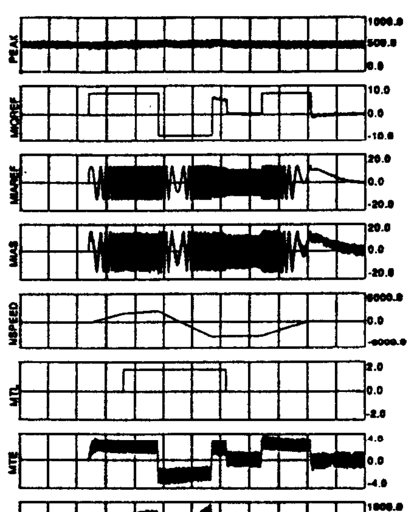

Fig 7. Dynamic Response of System During Speed Reversal and During Load Application and Removal. From the Top; **PEAK:** Peak of the HF Link Voltage-V. **MIQREF:** Induction Motor Torque Component Current Command-A. **MIAREF:** Motor Phase-A Line Current Reference-A. **MIAS:** Induction Motor Phase-A Line Current-A. **MSPEED:** Speed of Motor-rpm. **MTL:** Load Torque Applied to Induction Motor-Nm. **MTE:** Average Motor Torque-Nm. **POUT:** Average Output Power of MotorW. Time/div: 83.333 msec.

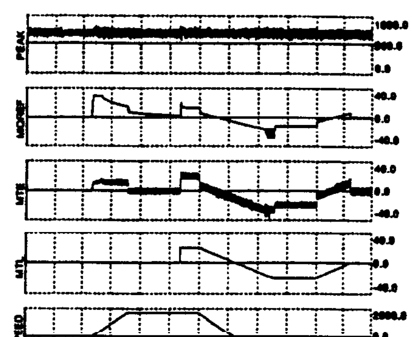

Fig 8. Dynamic Response of Induction Motor and Overall System to Speed and Load Torque Changes with 10 HP Induction Motor. From the Top; **PEAK:** Peak of the HF Link Voltage-V. **MIQREF:** Motor Torque Component Current Command-A. **MTE:** Average Motor Electrical Torque-Nm. **MTL:** Motor Load Torque-Nm. **MSPEED:** Speed of Induction Motor-rpm. **MSPREF:** Speed Reference of Induction Motor-rpm. Time/div: 125 msec.

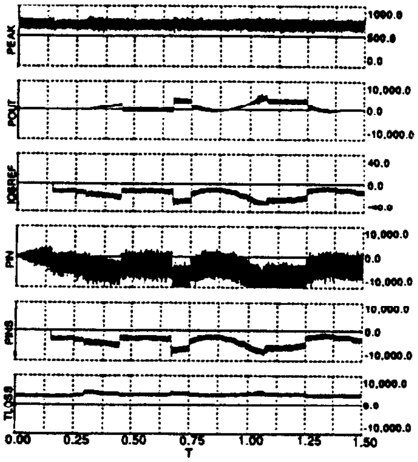

Fig. 9. Dynamic Response of Induction Motor and System to Speed and Load Torque Changes with 10 HP Induction Motor. From the Top: **PEAK:** Peak of the HF Link Voltage-V. **TLOSS:** Total Loss of the Resonant Tank and PDM Converter-W. **IQSREF:** Generator Torque Component Current Command in A. **POUT:** Average Output Power of Induction Motor in W. **PINS:** Estimated Average Generator Power-W. **PIN:** Average Generator Power-W. Time/div: 125 msec.

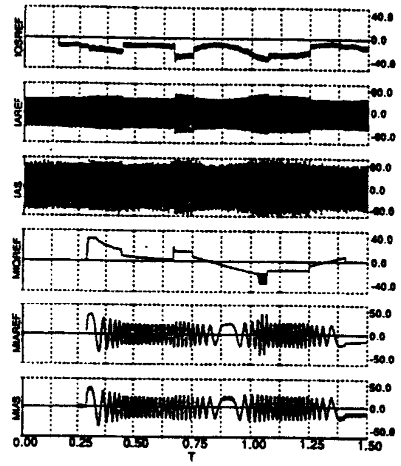

Fig. 10. Dynamic Response System to Speed and Load Torque Changes Using 10 HP Induction Motor. From the Top: **IQSREF:** Induction Generator Torque Component Current Command-A. **IASREF:** Generator Phase A Line Current Reference-A. **IAS:** Induction Generator Phase-A Line Current-A. **MIQREF:** Motor Torque Component Current Command-A. **MIASREF:** Induction Motor Phase-A Line Current Reference-A. **MIAS:** Induction Motor Phase-A Line Current-A. Time/div: 125 msec.

The proposed system offers fast dynamic response, full four quadrant operation, bidirectional power flow and as well as low harmonic distortion of the input and output signals for the control of associated induction machines. The system, being completely isolated from other sources of reactive energy lends itself easily to typical space station utility interface applications because of the tendency of the system to realize higher power densities and greater flexibility of ac link to voltage requirements.

References

[1] T. A. Lipo and P. K. Sood, *Feasibility Study of an Induction Generator System Employing a Bi-Directional Resonant Converter for Aircraft Power Supply*, Final Report, NASA Grant NAG3-492, April 4, 1986.

[2] T. A. Lipo and P. K. Sood, *Study of the Generator/Motor Operation of Induction Machine in a High Frequency Link Space Power System*, NASA Contractor Report, Contract No. NAG 631, March, 1987.

[3] T. A. Lipo and S. K. Sul, *Design and Test of Bidirectional Speed and Torque Control of Induction Machines Operating from High Frequency Link* April, *Converter*. Final Report, NASA Contract NAG3-786, 1988.

[4] P.K. Sood and T.A. Lipo, *Power Conversion Distribution System Using a Resonant High-Frequency AC Link*, IEEE Trans. on Industry Applications, vol. 24, Mar/Apr. 1988, pp. 288-300.

[5] P. Sood, T.A. Lipo and I. Hansen, *A Versatile Power Converter for High Frequency Link Systems*, IEEE Trans. on Power Electronics, vol. 3, No. 4, Oct. 1988, pp. 383-390.

[6] S.K. Sul and T.A. Lipo, *Design and Performance of a High Frequency Link Induction Motor Drive Operating at Unity Power Factor*, 1990 IEEE Trans. on Industry Applications, Vol. 26, No. 3, May/June 1990, pp. 434-440.

[7] S.K. Sul and T.A. Lipo, *Field Oriented Control of an Induction Machine in a High Frequency Link Power System*, IEEE Trans. on Power Electronics, vol 5, No. 4, October 1990, pp. 436-445.

[8] S.K. Sul, F. Profumo, G.H. Cho and T.A. Lipo, *MCTs and IGBTs: A Comparison of Performance in Power Electronics Circuits*, 1989 IEEE Power Electronics Specialists' Conference, June 26-29, 1989, pp. 163-169.

[9] S.K. Sul, I. Alan and T.A. Lipo, *Performance Testing of a High Frequency Link Converter for Space Station Power Distribution System*, 1989 Intersociety Energy Conversion Engineering Conference, Washington DC, August 1989, vol. 1, Aerospace Power systems and Power Conditioning, pp. 617-624.

[10] T.A. Lipo and I. Alan, *System and Component Design and Test of a 10 HP, 18,000 RPM AC Dynamometer Utilizing a High Frequency AC Voltage Link*, Final Report, Contract No. NAG3-940, June 1991.

[11] I. Alan, *Three Phase to Three Phase Power Conversion Based Upon Parallel Resonant High Frequency AC Link*, Preliminary Thesis Proposal, Department of Electrical and Computer Engineering, University of Wisconsin-Madison, August, 1991.